

Generalisation of Recurrence Plot Analysis for Spatial Data

Norbert Marwan[†] and Peter Saparin[‡] and Jürgen Kurths[†]

[†]University of Potsdam, Institute of Physics, Nonlinear Dynamics Group
14415 Potsdam, Germany

[‡]Max Planck Institute of Colloids and Interfaces, Department of Biomaterials
14424 Potsdam-Golm, Germany

Email: marwan@agnld.uni-potsdam.de, peter.saparin@mpikg.mpg.de

Abstract—The method of recurrence plots and algorithms for their quantification are extended to analyse spatial data thus allowing to study recurrent structures in 2D images. To verify its capabilities, the method is tested on prototypical 2D models. Next, the developed approach is applied to assess the bone structure from CT images of human proximal tibia. It is found that the spatial structures in trabecular bone become more self-similar during the bone loss in osteoporosis.

1. Introduction

Recurrence is a fundamental property of various dynamical processes in nature. The investigation of recurrent behaviour can help to reveal dynamical properties of the system and to predict its states in the future. In order to study of nonlinear chaotic systems, several methods for the investigation of recurrences were developed. In 1987, Eckmann et al. introduced *recurrence plots* (RPs) for visualisation of phase space trajectories [2]. Together with different quantification approaches [6, 11], this method has been known in a growing scientific community.

RP based methods are successfully applied to a wide class of data and signals, e.g., from life and Earth sciences. They are especially suitable for the investigation of short and “nonstationary” data. This method works with time series or data, which are at least presented by one-dimensional (1D) series. However, recurrences occur not only in the time domain of processes; spatial objects can also exhibit typical recurrent structures. However, in their present state, RPs cannot be directly applied to spatial (or any other higher-dimensional) data. In order to study spatial recurrences, the method of RPs has to be extended.

In the following, we will present a possibility to analyse spatial recurrences. For this purpose, we extend the existing method of recurrence plots and their quantification to evaluate 2-dimensional (2D) data. This extension enables 2D image analysis with RPs. We apply this method to Peripheral Quantitative Computed Tomography (pQCT) images of bone in order to investigate differences in trabecular bone structures at different stages of osteoporosis.

2. Recurrence Plots

2.1. Definition

The main intention for introducing recurrences plots (RPs) was to visualize the behaviour of m -dimensional phase space trajectories $\vec{x}_i \in \mathbb{R}^m$ [2]. An RP is a graphical representation of such points in time, when the trajectory recurs in an ε -neighbourhood to a former state. A recurrence of a state at time i at a different time j is pictured within a 2D squared matrix with black and white dots, where black dots mark recurrence, and both axes are time axes (Fig. 1). This can be mathematically expressed as

$$R_{i,j} = \Theta(\varepsilon - \|\vec{x}_i - \vec{x}_j\|), \quad \vec{x}_i \in \mathbb{R}^m, \quad i, j = 1 \dots N, \quad (1)$$

where N is the number of considered states \vec{x}_i , ε is a threshold distance, $\|\cdot\|$ a norm and $\Theta(\cdot)$ the Heaviside function.

It should be emphasized that this method is a pairwise test of states on a trajectory which is – although lying in an m -dimensional space – a 1D object. The axes of the RP correspond with the time which is given by pursuing a state on the trajectory. From Eq. (1) it is obvious that the RP is symmetric.

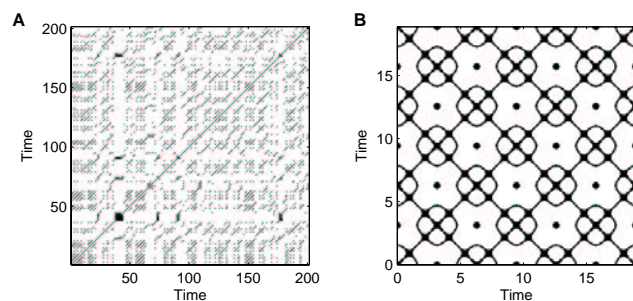


Figure 1: (A) Exemplary recurrence plot for the logistic map $x_{i+1} = ax_i(1 - x_i)$ with $a = 3.87$, representing single dots and line structures as typical for chaotic systems. (B) Recurrence plot of superpositioned harmonic oscillations ($f(x) = \sin(x) \sin(x/2)$), representing periodically occurring diagonal lines.

Table 1: Several recurrence quantification measures [6, 11].

| RQA measure | equation | meaning |
|-------------------------------|---|--|
| recurrence rate | $RR = \frac{1}{N^2} \sum_{i,j=1}^N \mathbf{R}_{i,j}$ | percentage of recurrent states in the system; probability of the recurrence of any state |
| determinism | $DET = \frac{\sum_{l=l_{min}}^N l P(l)}{\sum_{i,j} \mathbf{R}_{i,j}}$ | percentage of recurrence points which form diagonal lines; related with the predictability of the system |
| laminarity | $LAM = \frac{\sum_{v=v_{min}}^N v P(v)}{\sum_{v=1}^N v P(v)}$ | percentage of recurrence points which form vertical lines; related with the laminarity of the system |
| averaged diagonal line length | $L = \frac{\sum_{l=l_{min}}^N l P(l)}{\sum_{l=l_{min}}^N P(l)}$ | related with the predictability time of the system |
| trapping time | $TT = \frac{\sum_{v=v_{min}}^N v P(v)}{\sum_{v=v_{min}}^N P(v)}$ | related with the laminarity time of the system |

2.2. Quantification

An RP uncovers epochs of similar dynamical evolution of the considered system. For $i = j$, we get the *line of identity* (LOI) $\mathbf{R}_{i,i} = 1$, which is the main diagonal line in the RP (Fig. 1). For $i \neq j$, epochs of similar dynamical evolution with the duration l are represented as diagonal lines of length l

$$(1 - \mathbf{R}_{i+l,j+l}) \prod_{\lambda=0}^{l-1} \mathbf{R}_{i+\lambda,j+\lambda} \equiv 1. \quad (2)$$

An RP of a periodic process contains continuous diagonal lines with a periodic distance from each other (Fig. 1B). Moreover, an RP can also contain vertical (and horizontal) lines of length v , which represent states which do not change for some time v

$$(1 - \mathbf{R}_{i,j+v}) \prod_{\varphi=0}^{v-1} \mathbf{R}_{i,j+\varphi} \equiv 1. \quad (3)$$

These diagonal and vertical lines are the base for the quantification of RPs. Using the distributions of the lengths of diagonal lines $P(l)$ and vertical lines $P(v)$, different measures of complexity were introduced (detailed definitions and descriptions of these measures can be found in [4]). Here we focus on the recurrence rate RR , determinism DET , averaged diagonal line length L , laminarity LAM and trapping time TT (Tab. 1).

For the definition of a diagonal or vertical line, several measures need a predefined minimal length l_{min} or v_{min} , respectively. These minimal lengths should be as minimal as possible, but large enough to exclude line-like structures which represent only single, non-recurrent states, which may occur if the threshold ε is chosen too large or the data are rather smooth.

These measures help to find transitions in data series [6, 10] or to study interrelations between different systems [5]. Using the distributions of the diagonal line lengths, basic dynamical invariants, like K_2 entropy, can be estimated [9].

2.3. Extension to two dimensions

Now we propose an extension of RPs to spatial (2D) data. With this step we leave the field of deterministic dynamical systems and focus on the potential of the RPs in identification of similar (recurrent) features in spatial data.

For a 2D (cartesian) system of size $N_1 \times N_2$, we extend the recurrence plot to

$$\mathbf{R}_{i_1,i_2,j_1,j_2} \equiv \Theta(\varepsilon - \|x_{i_1,i_2} - x_{j_1,j_2}\|), \quad i_{1,2}, j_{1,2} = 1 \dots N_{1,2}. \quad (4)$$

Thus, we consider each spatial direction as a single 1D data series, but compare each of them with all others. The resulting RP has now the dimension 4 and cannot be visualised anymore, but its quantification is still possible.

Analogous to the 1D case, where the LOI $\mathbf{R}_{i,i} \equiv 1 \forall i = j$ is a 1D line, we define a diagonal oriented, 2D structure in the 4D recurrence plot, the *surface of identity* (SOI): $\mathbf{R}_{i_1,i_2,i_1,i_2} \equiv 1$, which is in fact a 2D plane.

2.4. Quantification of higher-dimensional RPs

Because the recurrence quantification is based on diagonal and vertical line structures in RPs, the definition of equivalent structures in the 4D RP is crucial for its quantification analysis. Analogous to the definition of diagonal and vertical lines, Eqs. (2) and (3), we define a diagonal squared surface of size l^2 by

$$(1 - \mathbf{R}_{i_1+l,i_2+l,j_1+l,j_2+l}) \prod_{\lambda_1,\lambda_2=0}^{l-1} \mathbf{R}_{i_1+\lambda_1,i_2+\lambda_2,j_1+\lambda_1,j_2+\lambda_2} \equiv 1, \quad (5)$$

and a vertical squared surface of size v^2 by

$$(1 - \mathbf{R}_{i_1,i_2,j_1+v,j_2+v}) \prod_{\varphi_1,\varphi_2=0}^{v-1} \mathbf{R}_{i_1,i_2,j_1+\varphi_1,j_2+\varphi_2} \equiv 1. \quad (6)$$

Using these definitions, the frequency distributions $P(l)$ and $P(v)$ of the sizes of diagonal and vertical surfaces in the RP can be calculated. The recurrence quantification measures, as defined in Tab. 1, can then be applied to these

distributions, thus, these quantification measures are now suitable for characterizing 2D spatial data. In the following we apply the proposed spatial recurrence analysis on prototypical examples and 2D images of human bone.

3. Applications

3.1. Example

At first, we consider three 2D model examples. The first image (A) is uniformly distributed white noise, the second (B) is produced by a 2D linear auto-regressive process of 2nd order (2D-AR2) and the third (C) represents periodically recurrent structures (Fig. 2). All these examples have a geometric extension of 200×200 pixels² and their pixel values were normalized to a mean of zero and a standard deviation of one.

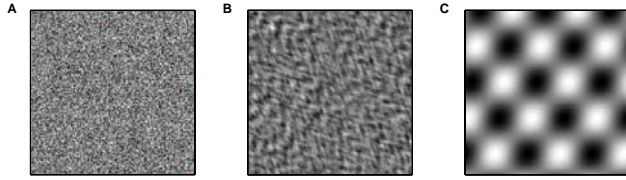


Figure 2: 2D examples representing (A) uniformly distributed white noise, (B) a 2D auto-regressive process and (C) periodically recurrent structures.

The resulting RPs are 4D matrices of size 200^4 , and can hardly be visualized. Next, we compute the recurrence quantification measures as defined in Sec. 2.4 for the size distributions of diagonal and vertical planes in the 4D RPs. We use a threshold $\varepsilon = 0.2$, and for the minimal size of the diagonal and vertical planes $l_{min} = 3$ and $v_{min} = 4$.

Except the recurrence rate RR , the recurrence quantification measures discriminate significantly between the structures in the three examples (Tab. 2). RR is roughly the same for all examples. This is because all images were normalized to the same standard deviation and all pixel values occur equally frequent in all three images. For the random image (A), the determinism DET and laminarity LAM tend to zero, as expected, because the pixel values heavily fluctuate even between adjacent pixels. For the 2D-AR2 image (B), DET and LAM are slightly above zero, revealing the correlation between adjacent pixels. The last example (C) has, as expected, the highest values in DET and LAM , because same structures occur many times in this image. Although the trend of DET and LAM seems to be similar, there is a significant difference between both measures. Whereas LAM represents the probability that a specific value will not change over spatial variation (what results in extended same-coloured areas in the image), DET measures the probability that similar changes in the image recur. LAM is twice of DET for the 2D-AR2 image, revealing that there are more extended areas with same pixel values in the image than such areas where pixel values change

in a similar way. These examples show that the proposed spatial recurrence analysis can reveal and quantify spatially recurrent structures. Next we try to uncover such recurrent structures in 2D pQCT data of bone of different stages of osteoporosis.

Table 2: Recurrence quantification measures for prototypical 2D examples.

| Example | RR | DET | LAM | L | TT |
|--------------|-------|-------|-------|-----|------|
| (A) noise | 0.218 | 0.007 | 0.006 | 3.7 | 3.0 |
| (B) 2D-AR2 | 0.221 | 0.032 | 0.065 | 3.1 | 3.1 |
| (C) periodic | 0.219 | 0.322 | 0.312 | 5.8 | 5.6 |

3.2. pQCT data of proximal tibia

Osteoporosis is a disease characterized by bone loss and changes in the bone structure. In the last years, the focus changed to structural assessment of the trabecular bone, because bone densitometry alone cannot explain all variation in bone strength. Furthermore, the rapid progress in the development of new high-resolution CT scanners facilitates investigations of the bone micro-architecture. Different approaches using methods coming from nonlinear dynamics were recently proposed in order to evaluate structural changes [1, 8] or even to predict fracture risks or biomechanical properties of bones [3, 7]. These approaches use e.g. fractal properties or complexity of trabecular network. Using the RP based method, we will focus on the recurrent structures and their extensions obtained from a pQCT images of trabecular bone at different stages of osteoporosis as assessed by bone mineral density (BMD). Being applied to such images, RP provides information about recurrences of bone and soft tissue.

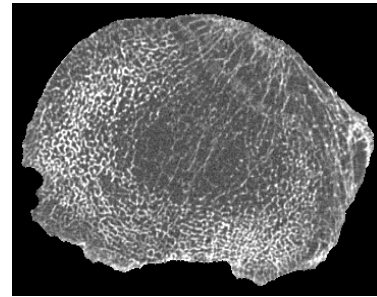


Figure 3: Axial pQCT slice of human proximal tibia acquired 17 mm below the tibial plateau. The BMD is 65.5 mg/cm^3 .

The spatial recurrence analysis is applied to high-resolution pQCT axial slices of human proximal tibia, pixel size $200 \mu\text{m}$, slice thickness 1 mm (Fig. 3). The images were acquired from 26 bone specimens with a pQCT scanner XCT-2000 from Stratec GmbH, Germany. The trabecular bone mineral density of these specimens ranges from 0 to 150 mg/cm^3 . A standardized image pre-processing

was applied to exclude the cortical shell from the analysis [8]. The RP quantification was computed for $\varepsilon = 40$ HU, $l_{min} = 2$ and $v_{min} = 2$.

The new RP measures reveal a relationship between recurrent structures in pQCT images of trabecular bone and degree of osteoporosis, represented by the *BMD* (Fig. 4). *RR* increases for decreasing *BMD*. Spearman's rank order correlation coefficient *R* between *RR* and *BMD* is -0.95 . *DET* and *LAM* are less anti-correlated than *RR* ($R_{DET} = -0.69$, $R_{LAM} = -0.80$). With decreasing bone mass, the spatially distributed structures in the corresponding pQCT image, which can be bone or marrow patterns, become more and more self-similar. This corresponds with our previous findings, that the complexity of the trabecular micro-architecture decreases during bone loss [8].

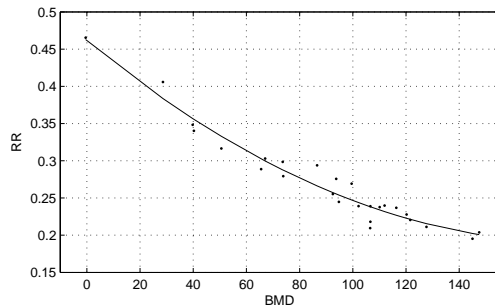


Figure 4: Recurrence rate obtained from 4D RPs of pQCT images of human proximal tibia of different osteoporotic stages.

The other measures *L* and *TT* are weakly anti-correlated with *BMD* ($R_L = -0.36$, $R_{TT} = -0.57$, resp.). The sizes of the recurrent structures do not change much during the development of osteoporosis.

3.3. Conclusions

Applying the proposed spatial extension of RPs we find that this method is able to reveal recurrent structures in 2D images. It can be used to quantify structures in medical CT images. This approach could provide a base for the development of a method for assessment of structural alteration in trabecular bone during the development of osteoporosis or in microgravity position. Presented results are work in progress and should be considered as preliminary.

Acknowledgments

This study was made possible in part by grants from project MAP AO-99-030 (contract 14592) of the Microgravity Application Program/Biotechnology from the Human Spaceflight Program of the European Space Agency (ESA). The authors would also like to acknowledge Scanco Medical, Siemens AG, and Roche Pharmaceuticals for support of the study. We thank Wolfgang Gowin and Erika May for preparation and scanning of the bone specimens.

References

- [1] C. L. Benhamou, E. Lespessailles, G. Jacquet, R. Harba, R. Jennane, T. Loussot, D. Tourliere, and W. Ohley. Fractal Organization of Trabecular Bone Images on Calcaneus Radiographs. *J. Bone Min. Res.*, 9(12):1909–1918, 1994.
- [2] J.-P. Eckmann, S. O. Kamphorst, and D. Ruelle. Recurrence Plots of Dynamical Systems. *Europhys. Lett.*, 5:973–977, 1987.
- [3] T. J. Haire, R. Hodgskinson, P. S. Ganney, and C. M. Langton. A comparison of porosity, fabric and fractal dimension as predictors of the young's modulus of equine cancellous bone. *Med. Eng. & Phys.*, 20(8):588–593, 1998.
- [4] N. Marwan. *Encounters With Neighbours – Current Developments Of Concepts Based On Recurrence Plots And Their Applications*. PhD thesis, University of Potsdam, 2003.
- [5] N. Marwan, M. H. Trauth, M. Vuille, and J. Kurths. Comparing modern and Pleistocene ENSO-like influences in NW Argentina using nonlinear time series analysis methods. *Clim. Dyn.*, 21(3–4):317–326, 2003.
- [6] N. Marwan, N. Wessel, U. Meyerfeldt, A. Schirdewan, and J. Kurths. Recurrence Plot Based Measures of Complexity and its Application to Heart Rate Variability Data. *Phys. Rev. E*, 66(2):026702, 2002.
- [7] S. Prouteau, G. Ducher, P. Nanyan, G. Lemineur, L. Benhamou, and D. Courteix. Fractal analysis of bone texture: a screening tool for stress fracture risk? *Eur. J. Clin. Inv.*, 34(2):137–142, 2004.
- [8] P. I. Sagarin, W. Gowin, J. Kurths, and D. Felsenberg. Quantification of cancellous bone structure using symbolic dynamics and measures of complexity. *Phys. Rev. E*, 58(5):6449, 1998.
- [9] M. Thiel, M. C. Romano, P. L. Read, and J. Kurths. Estimation of dynamical invariants without embedding by recurrence plots. *Chaos*, 14(2):234–243, 2004.
- [10] L. L. Trulla, A. Giuliani, J. P. Zbilut, and C. L. Webber Jr. Recurrence quantification analysis of the logistic equation with transients. *Phys. Lett. A*, 223(4):255–260, 1996.
- [11] C. L. Webber Jr. and J. P. Zbilut. Dynamical assessment of physiological systems and states using recurrence plot strategies. *J. Appl. Phys.*, 76(2):965–973, 1994.